Comparison of cyclic triaxial behavior of unbound granular material under constant and variable confining pressure

H. A. Rondón[i)] T. Wichtmann,[ii)] Th. Triantafyllidis,[iii)] A. Lizcano[iv)]

Abstract: Cyclic stresses due to passing wheels impose an accumulation of permanent strains in layers of unbound granular materials (UGMs) of flexible pavements. The hollow cylinder triaxial test would be the most appropriate test to simulate the in situ stress conditions but it is difficult to perform on UGMs due to their large maximum grain size. The simpler axi-symmetric cyclic triaxial test does not consider the shear stress components. It can be performed with a constant (CCP) or a variable confining pressure (VCP). CCP and VCP tests are commonly assumed to deliver similar residual and resilient strains as long as the average stress is the same. Thus, the simpler CCP test is mostly used in pavement engineering. However, this assumption is based on limited test data in the literature and may not be on the safe side. The present paper documents a comparative study of CCP and VCP tests on UGM. The study is mainly dedicated to the permanent deformations. The results show that only for some special stress paths both types of test deliver similar permanent axial or volumetric strains. For some other stress paths the CCP test may underestimate the permanent axial strain in comparison to the corresponding VCP test.

CE Database subject headings: Flexible pavements; Unbound granular material (UGM); Cyclic loading; CCP triaxial tests; VCP triaxial tests

1 Introduction

Many design procedures for pavements (e.g. [1,18,20,32,37, 43]) suppose that permanent deformations occur mainly in the subgrade. The behavior of base and subbase layers made of unbound granular materials (UGMs) is assumed linear or non-linear elastic. However, due to the large cyclic stresses occuring in the UGM layers of flexible pavements an inelastic portion of deformation accumulates with each cycle (e.g. [8, 15, 19, 45]). The settlements may become significant after a large number of cycles.

Starting in the 1960s significant research has been done on the resilient characteristics of UGM materials. Mathematical models for the prediction of the resilient modulus for different cyclic stress paths have been developed. The models assume isotropically (e.g. [9, 13, 27]) or anisotropically non-linear elastic (e.g. [3, 26, 52, 58]) or hyperelastic (e.g. [28, 51]) material behavior.

Permanent deformations of UGMs were less frequently studied than the resilient properties (e.g. [7, 15, 17, 22, 24, 25, 31, 38, 39, 50, 57, 59–61, 63]). Empirical or semi-empirical models for the prediction of permanent strains in dependence of stress (usually described by the confining pressure and the amplitude of the cyclic load) and the number of load cycles have been developed. A discussion of factors affecting the UGM behavior and a summary of the most important models can be consulted in [38] and [48]. However, in spite of a great amount of research, the complex behavior of UGMs is not totally understood yet. While a

satisfactory progress has been made in the prediction of the resilient behavior, the advances in the prediction of permanent strain accumulation were less significant [19].

One limitation is the lack of appropriate test devices to simulate the in situ stress paths in a pavement (Fig. 1). Ideally, in a laboratory element test the axial, the two lateral and the shear stress components should be controlled independently of each other. The device should be capable to simulate rotations of the principal stress directions. The most appropriate device to apply this loading would be the hollow cylinder apparatus [19,44,55]). However, its usage for tests on UGM is limited due to the large maximum grain size of such materials in comparison to the wall thickness of the hollow cylinder specimen. In true triaxial devices the three principal stresses can be controlled independently but their directions do not change. Most of the research on UGMs is made by means of axi-symmetric cyclic triaxial tests. Those tests are either performed with a constant (CCP) or with a variable (VCP) confining pressure. CCP tests simulate only the vertical component of the cyclic stresses. VCP tests are somewhat better since they simultaneously simulate vertical and lateral cyclic stresses. However, both types of tests cannot reproduce the shear stress component in addition to the normal stresses, which means that the rotation of the principal stress directions is not considered.

In comparison to CCP tests only a few studies with VCP tests have been performed due to different reasons. Test devices with the possibility to vary the confining pressure are less widespread than those for an application of axial cyclic loads. The loading frequencies in VCP tests are usually smaller than in CCP tests due to technical limitations. Thus, it takes longer time to reach a sufficiently large number of cycles. A variation of the confining pressure implicates the problem of membrane penetration [42], which means that complicated measurements of lateral de-

---

[i)] Research Assistant, Department of Civil and Environmental Engineering. Los Andes University, Bogotá D. C. (Colombia)

[ii)] Research Assistant, Institute of Soil Mechanics and Rock Mechanics, University of Karlsruhe, Germany (corresponding author). Email: torsten.wichtmann@ibf.uka.de

[iii)] Professor and Director of the Institute of Soil Mechanics and Rock Mechanics, University of Karlsruhe, Germany

[iv)] Professor, Department of Civil and Environmental Engineering. Los Andes University, Bogotá D. C. (Colombia)
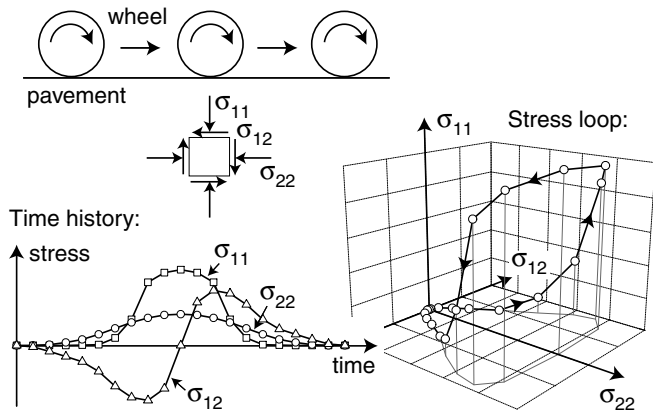
Fig. 1: Stress variation beneath a rolling wheel load [38]

formations directly on the specimen are indispensable (at least for studies of the resilient behaviour). Most of the empirical equations available for the prediction of permanent strain in an UGM were developed based on CCP triaxial test results (e.g. [7,30,31,50,57,60]).

In standard codes or design guidelines it is often assumed that CCP and VCP tests deliver similar results as long as the average stress is the same. Thus, for engineering applications it is easier to use the simpler CCP tests to quantify the permanent deformations. However, this assumption is based on a limited number of tests and thus it is questionable if it is on the safe side. Some comparative studies with CCP and VCP triaxial tests have been documented in the literature (e.g. [4,12,41,67]) but most of them have been concentrated on the resilient characteristics. Only some were dedicated to the permanent strains:

- Chan & Brown [16] compared CCP triaxial tests and hollow cylinder tests on a sand with a maximum grain size of 5 mm. In both types of tests the confining pressure was kept constant and the vertical stress was varied cyclically. The additional oscillation of shear stress in the hollow cylinder test lead to a larger rate of shear strain accumulation. Based on shaking table tests, multidimensional simple shear tests or VCP triaxial tests on sand also other researchers [34,46,65] demonstrated an increase of the accumulation rate with increasing number of oscillating stress or strain components (i.e. with increasing dimensionality of the cyclic stress or strain path). For example, Wichtmann et al. [65] observed approximately twice larger accumulation rates for a circular cyclic strain path compared to a one-dimensional strain path with an amplitude identical to the radius of the circles.

- Only a few comparative studies were performed on UGM. Although no attempts were made to quantify the permanent strains, Allen & Thompson [4] reported on larger permanent strains in CCP tests than in VCP tests. Allen & Thompson [4] compared the stress paths presented in Fig. 2a. The maximum stress (p^{max}, q^{max}) with the mean pressure $p = (\sigma_1 + 2\sigma_3)/3$ and with the deviatoric stress $q = \sigma_1 - \sigma_3$ was identical for the CCP and the VCP tests. Thus, both stress paths have the same amplitude of deviatoric stress $q^{ampl} = (q^{max} - q^{min})/2$ but different amplitudes of

mean pressure p^{ampl} and also different average mean pressures $p^{av} = (p^{min} + p^{max})/2$.
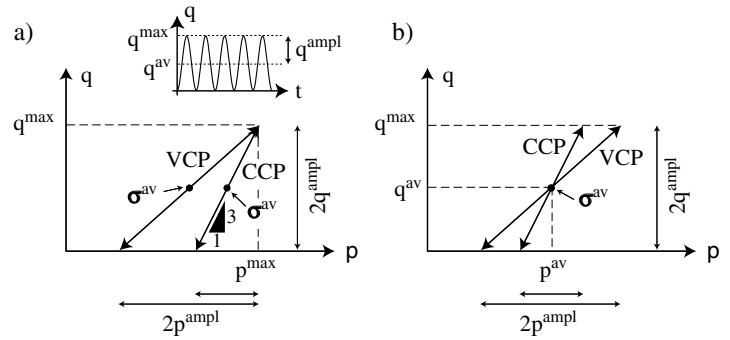

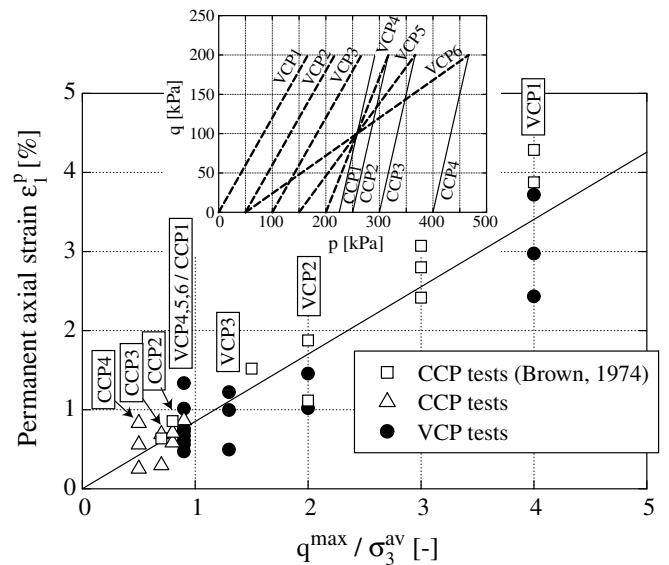Fig. 2: Scheme of stress paths used a) by Allen & Thompson [4] and b) recommended by Brown & Hyde [12]

Fig. 3: Tests of Brown & Hyde [12]: Permanent axial strain versus the ratio of the maximum deviatoric stress q^{max} and the average confining pressure σ_3^{av}

- Brown & Hyde [12] argued that a comparison of cyclic stress paths with an identical average stress, (i.e. identical values of p^{av} and q^{av}, as shown in Fig. 2b) is more meaningful. In such a case the CCP and VCP stress paths are the same except for the amplitude p^{ampl}. Brown & Hyde tested an UGM under the stress paths shown in Fig. 3. The test data was supplemented by data from an older CCP test series [11]. In Fig. 3 the residual axial strain ε_1^p is plotted versus the ratio q^{max}/σ_3^{av}. Since for same values of q^{max}/σ_3^{av} the data of CCP and VCP tests did not differ much, Brown & Hyde concluded that the accumulation of permanent strain is similar for the two types of tests. However, the scatter of data for $q^{max}/\sigma_3^{av} = 4$ is significant in Fig. 3 and the CCP tests seem to deliver larger strain accumulation rates. Furthermore, the tests of Brown & Hyde were restricted to a single value of $q^{max} = 200$ kPa.

If CCP and VCP triaxial tests are equivalent with respect to the accumulation of permanent strain, as long as

Index property	Value
Maximum grain size, $d_{\max}$ [mm]	16
Mean grain size, d_{50} [mm]	6.3
Coefficient of uniformity, $C_u = d_{60}/d_{10}$	100
Specific weight, ϱ_s [g/cm³]	2.65
Maximum dry density, $\varrho_{d,\max}$ [g/cm³]	2.16
Minimum dry density, $\varrho_{d,\min}$ [g/cm³]	1.84
Maximum void ratio, $e_{\max}$	0.44
Minimum void ratio, $e_{\min}$	0.23
Maximum proctor density, ϱ_{Pr} [g/cm³]	2.30
Optimum water content, w_{opt} [%]	5.2
Critical friction angle, φ_c [°]	38.0
Grain shape	Subangular

Table 1: Index properties of the tested UGM

the average confining stress σ_3^{av} and the amplitude of deviatoric stress q^{ampl} are the same in both types of tests, seems not fully clearified yet. This paper intends to make a contribution to this open question. It presents a study comparing the results of CCP and VCP tests, similar to the one performed by Brown & Hyde [12], but with a wider range of deviatoric stress amplitudes q^{ampl}. It shows that only for some special stress paths both types of test deliver similar permanent axial or volumetric strains.

2   Tested material

The grain size distribution curve (Fig. 4) used in the tests is in accordance with the Colombian Specification [20] for base layer construction in flexible pavements except for the maximum grain size. It was reduced to $d_{\max} = 16$ mm in order not to fall below a ratio $b/d_{\max}$ of 5 with $b \times b$ being the dimensions of the specimen cross section in the triaxial tests. This grain size distribution curve was mixed from different gradations of a natural quartz sand with subangular grain shape. For the fine particles a quartz meal was used. The index properties of the tested material are summarized in Table 1. A Proctor test with modified energy ($E = 2700$ kNm/m³) resulting in a maximum dry density $\varrho_{\mathrm{Pr}} = 2.30$ g/cm³ and an optimum water content $w_{\mathrm{opt}} = 5.2$ % has been presented by Rondón et al. [49]. The critical friction angle $\varphi_c = 38.0°$ has been determined as the inclination of a pluviated cone of the dry material.
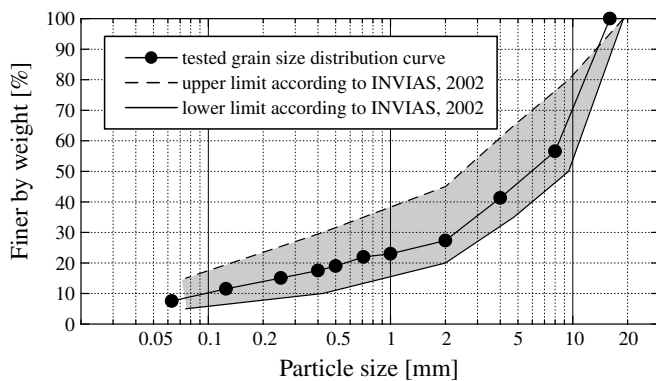

Fig. 4: Grain size distribution curve of the tested UGM compared to the limits of Colombian Specification (INVIAS [20])

3   Test device and specimen preparation

A scheme of the used triaxial device is given in Fig. 5. The cyclic axial load was applied with a pneumatic loading system and also the confining pressure could be cyclically varied by means of a pneumatic valve.
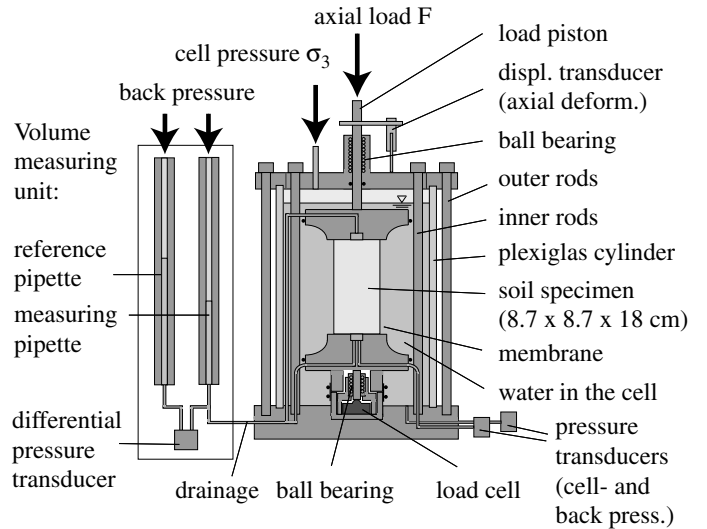

Fig. 5: Scheme of the used triaxial device

The prismatic specimens had dimensions $8.7 \times 8.7 \times 18$ cm. Specimens with a square cross section were used in order to measure lateral (and also axial) deformations locally by means of local displacement transducers (LDTs). Local measurements of lateral deformations are indispensable in VCP tests in order to get an information about the resilient behavior which is free from membrane penetration effects (Nicholson et al. [42]). In contrast, the CCP test results and also the permanent deformations in the VCP tests are not falsified by membrane penetration effects.

The LDTs are strips of phosphor bronze applied with strain gauges (see also Goto et al. [23], Hoque et al. [29]). In order to mount an LDT two hinges are glued to the membrane of the specimen. The LDT is placed between these hinges in an initially bended condition (Fig. 6g,h). The lateral deformation of the specimen between the two fixing points of the LDT is measured as a change of the bending of the LDT. Unfortunately, the LDTs available for the present study could not be used in combination with water in the cell. However, for the long-term cyclic triaxial tests the water in the cell is indispensable. Thus, a two-step testing program was chosen. The cyclic CCP and VCP triaxial tests were performed without LDT measurements. Afterwards, two additional short-term tests with LDT measurements were performed in which all CCP and VCP stress paths were applied in succession. The testing program is explained in detail in a following section.

The axial load was measured inside the pressure cell with a load cell located below the bottom end plate. The axial deformation was obtained from a displacement transducer attached to the load piston (Fig. 5). The system compliance was determined in preliminary tests on a dummy specimen. It was subtracted from the measured displacement. Volume changes were measured via the pore water of the fully saturated specimens using a pipette system and a differential pressure transducer. Deviations between the corrected total measurements and the local LDT measure-

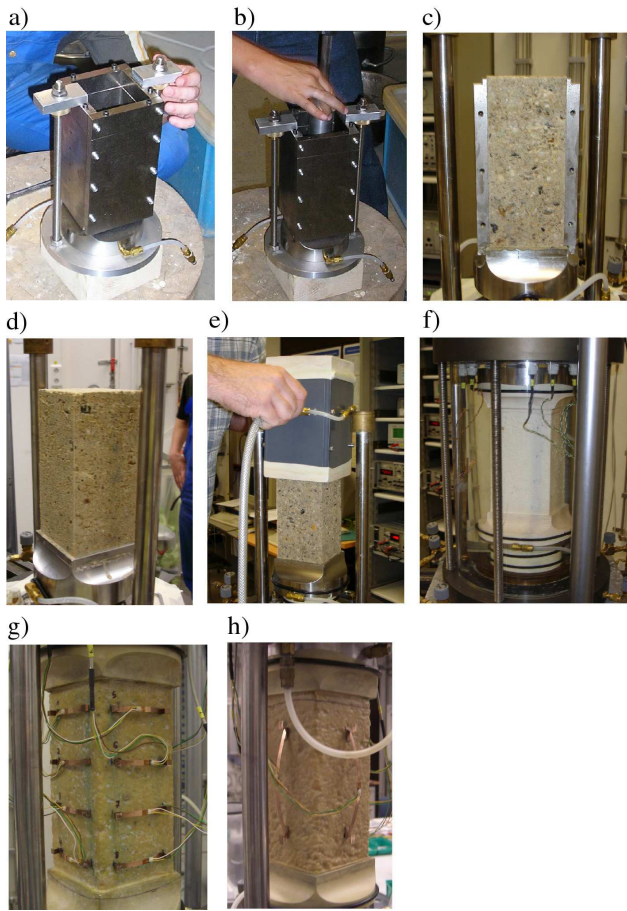ments of deformations are discussed later in this paper.

Fig. 6: Preparation of an UGM specimen for triaxial tests: a) Steel mould fixed to the bottom end plate of the triaxial cell (preparation outside the device), b) Moist tamping of the specimen with a miniature proctor hammer, c) Specimen after removal of one side of the mould, d) Specimen after removal of all sides of the mould, e) Placement of the membrane with a special stretcher, f) Specimen in the mounted triaxial cell prior to testing, g),h) Specimen equipped with local displacement transducers (LDTs, eight for the lateral and two for the axial direction)

For the specimen preparation a steel mould consisting of four plates was fixed to the bottom end plate of the triaxial cell (Fig. 6a). The specimen preparation was performed outside the triaxial cell in order to preserve the load cell. Specimens were prepared by tamping in $n = 6$ layers each with a thickness of 3 cm. The material was in the moist condition (water content $w = w_{\text{opt}} = 5.2$ %). A miniature proctor hammer (Fig. 6b) was used. Its fall weight ($m = 1$ kg, i.e. $G = 10$ N) was dropped from a height of $H = 20$ cm and $N = 250$ blows were applied to each layer. An energy per volume (total volume of a specimen $V = 1362$ cm^3) in the order of magnitude of $E = N \cdot n \cdot G \cdot h/V \approx 2200$ kNm/m^3 was induced into a specimen. It was chosen lower than the energy used in the modified Proctor test in order to reach densities slightly lower than the modified Proctor density (93 - 96 % of ϱ_{Pr}), which are typical for UGM layers in situ. After the tamping procedure the bottom end plate with the mould and the specimen was placed into the triaxial cell and the mould was removed (Figures 6c,d). The specimen stands due to

capillary pressure. Afterwards the membrane was placed using a stretcher with square cross section (Fig. 6e). The specimen end plates have a special shape at the transition from the square to the round cross section. The round cross section is necessary to enable a proper sealing of the membrane by O-rings. Fig. 6f presents a specimen after the top plate was placed, the membrane was sealed, the triaxial cell was mounted and filled with water and the cell pressure was applied. Finally, the specimens were saturated with de-aired water. A back pressure of 200 kPa was used in all tests in order to improve saturation. The saturation was controlled by Skempton's B-Value. In all tests $B > 0.95$ was achieved.

Fig. 6g,h presents a specimen equipped with LDTs. On two adjacent sides of the specimen four LDTs were mounted horizontally for local measurements of the lateral deformation (Fig. 6g). The other two sides were equipped with LDTs mounted vertically for local measurements of the axial deformation (Fig. 6h).

Despite its extensive use (mainly in Japanese soil mechanics laboratories) specimens with a square cross section are sometimes set into question because an inhomogeneous deformation is expected. Surprisingly, experimental studies comparing a circular and a square cross section can hardly be found in the literature. Thus, prior to the tests on the UGM material, results of prismatic and cylindrical specimens have been compared for similar test conditions in monotonic [49] and cyclic triaxial tests on a medium coarse quartz sand. In both types of tests the material behavior did not depend on the geometry of the specimen. Thus, the use of prismatic specimens does not imply any disadvantages in comparison to cylindrical ones.

4   Monotonic triaxial tests

For the determination of shear strength parameters, three monotonic triaxial tests on specimens with large initial densities (relative density index $I_{D0} = (e_{\max} - e_0)/(e_{\max} - e_{\min})$ = 1.06 - 1.13, dry density > 95% of ϱ_{Pr}) were performed. The effective lateral stresses were $\sigma_3 = 50$, 100 and 200 kPa. The curves $q(\varepsilon_1)$ and $\varepsilon_v(\varepsilon_1)$ are given in Fig. 7. A peak friction angle $\varphi_{\text{Peak}} \approx 54°$ was determined (Rondón et al. [49]).

5   Testing program of the cyclic triaxial tests

Table 2 and Fig. 8 present the stress paths applied in the cyclic tests. Five pairs of VCP and CCP stress paths with identical p^{av}, q^{av} and q^{ampl} were tested. All VCP and CCP stress paths start from $q^{\min} = 0$. The VCP stress paths have a low minimum mean pressure $p^{\min} = 20$ kPa in order to simulate realistic in situ stress conditions for pavements. Three different inclinations $\eta^{\text{ampl}} = q^{\text{ampl}}/p^{\text{ampl}} = 0.75$, 1.125 and 1.5 of the VCP stress paths in the p-q-plane were tested.

The critical state line (CSL) in Fig. 8 was plotted with an inclination $M_c = 6 \sin \varphi_c/(3 - \sin \varphi_c) = 1.55$ using $\varphi_c = 38.0°$ (Table 1) determined for the dry material deposited by pluviation. The final stage of the monotonic tests (Fig. 7) may indicate that the critical stress ratio of the pre-compacted UGM is larger. For example, the stress ratio at the end of the test with $\sigma_3 = 200$ kPa was $\eta \approx 1.9$. In that case even the stress path of test CCP5 would completely lay below the CSL.

The loading frequency f was 0.05 Hz in the VCP tests

Wichtmann & Triantafyllidis

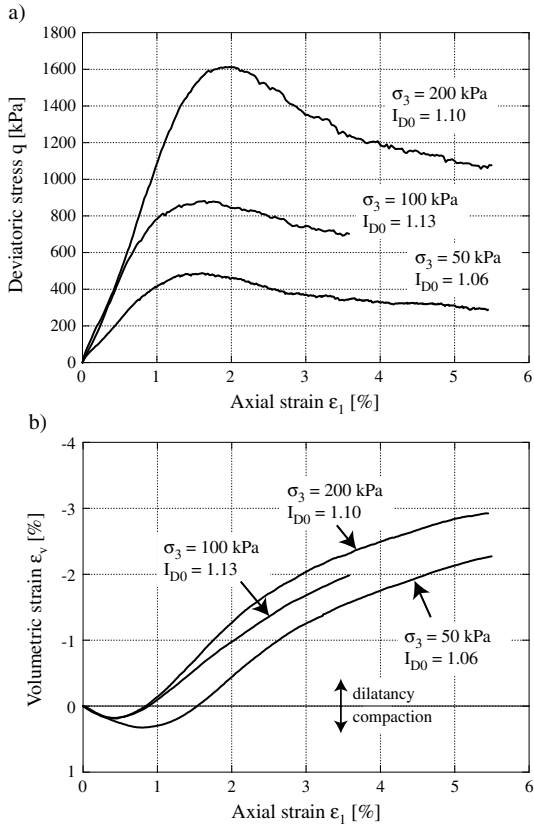J. Transp. Eng., ASCE, Vol. 135, No. 7, pp. 467-478, 2009

Fig. 7: Results of monotonic triaxial tests with different confining pressures: a) q vs. ε_1 and b) ε_v vs. ε_1
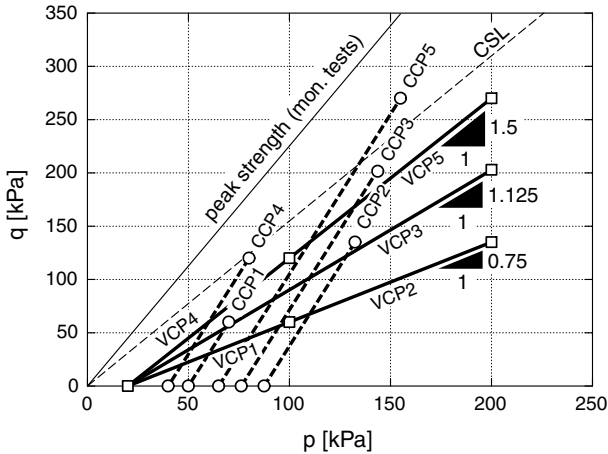

Fig. 8: VCP and CCP stress paths used for the present study

and 1 Hz in the CCP tests. The low frequency in the VCP tests was chosen due to technical limitations. Numerous researchers have reported on a negligible influence of the loading frequency on the resilient characteristics and on the permanent strain accumulation in sand (e.g. [64, 66]) or UGM (e.g. [4, 10, 11, 35, 47, 53, 54]). In order to prove the frequency-independence and in order to check the repeatability of the tests, four preliminary CCP tests were performed on the UGM (tests CCP2a to CCP2d, see Table 2). Either $3 \cdot 10^4$ cycles with $f = 0.05$ Hz or $2 \cdot 10^5$ cycles with $f = 1$ Hz were applied. Fig. 9 presents the curves of permanent axial strain ε_1^P versus the number of cycles N.

It shows no significant influence of the loading frequency and a satisfying reproducibility of the tests.
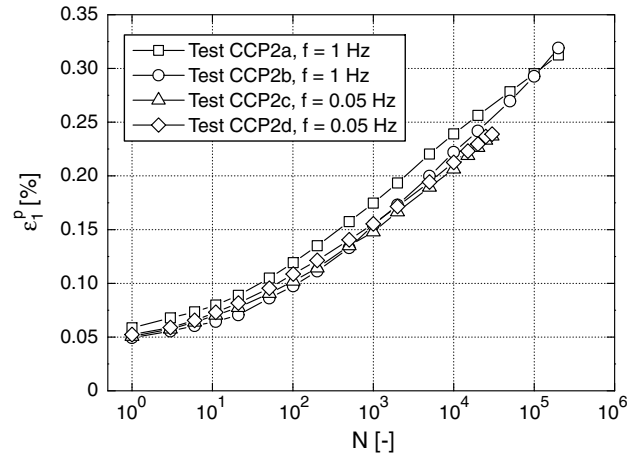

Fig. 9: Curves $\varepsilon_1^p(N)$ in preliminary tests: No influence of the loading frequency f and satisfying repeatability of the tests

Two additional tests were conducted with LDT measurements. These tests were performed without water in the cell. The lateral stress was applied via air pressure. In order to keep the specimens saturated, water was flushed through the specimen from time to time. After a large cyclic preloading (as recommended in [2] for studies of the resilient response); 20,000 cycles with the stress path of test CCP5, see Fig. 8, were applied) all stress paths of the CCP and VCP triaxial tests were applied in succession. The two tested specimens had similar initial densities as the specimens in the long-term cyclic tests. The same test was performed twice in order to check the repeatability.

6 CCP test results

Fig. 10a,b presents the curves of the axial permanent strain ε_1^p and of the volumetric permanent strain ε_v^p versus the number of cycles N in the CCP tests. While for small ratios $q^{\max}/\sigma_3^{\mathrm{av}}$ (tests CPP1 and CPP2) the residual strains grow almost proportional to $\ln(N)$, the curves show a steeper rise for larger stress ratios (tests CPP3 - CPP5). However, the inclination of the curves $\varepsilon_1^p(N)$ and $\varepsilon_v^p(N)$ in the semi-logarithmic scale decreases again for large numbers of cycles ($N > 10^5$).

Fig. 10c,d shows that ε_1^p and ε_v^p increase with the ratio $q^{\max}/\sigma_3^{\mathrm{av}}$. The wide-spread empirical function $\varepsilon_1^p = c_1(q^{\max}/\sigma_3^{\mathrm{av}})^{c_2}$ can be fitted to the test data (solid curves in Fig. 10c,d), wherein the parameters c_1 and c_2 could be formulated as functions of N. However, such empirical formulas are not the scope of the present study. Similar relationships $\varepsilon_1^p \sim q^{\max}/\sigma_3^{\mathrm{av}}$ have been reported by several other researchers, e.g. [5–7,11,14,21,33,36,39,40,56,61–63].

The permanent deviatoric strain $\varepsilon_q^p = 2/3(\varepsilon_1^p - \varepsilon_3^p)$ is plotted versus the permanent volumetric strain ε_v^p in Fig. 10e. The inclination of the ε_q^p-ε_v^p-strain paths (i.e. the ratio $\varepsilon_q^p/\varepsilon_v^p$) increases with increasing average stress ratio $\eta^{\mathrm{av}} = q^{\mathrm{av}}/p^{\mathrm{av}}$ of a test. These findings are concordant with test results on sand specimens [64]. However, while for sand a pure volumetric accumulation (i.e. $\dot{\varepsilon}_q^p = 0$ with the rate defined as $\dot{\sqcup} = \partial\sqcup/\partial N$) was observed for stress cycles with $\eta^{\mathrm{av}} = 0$, in the present tests on UGM the condition

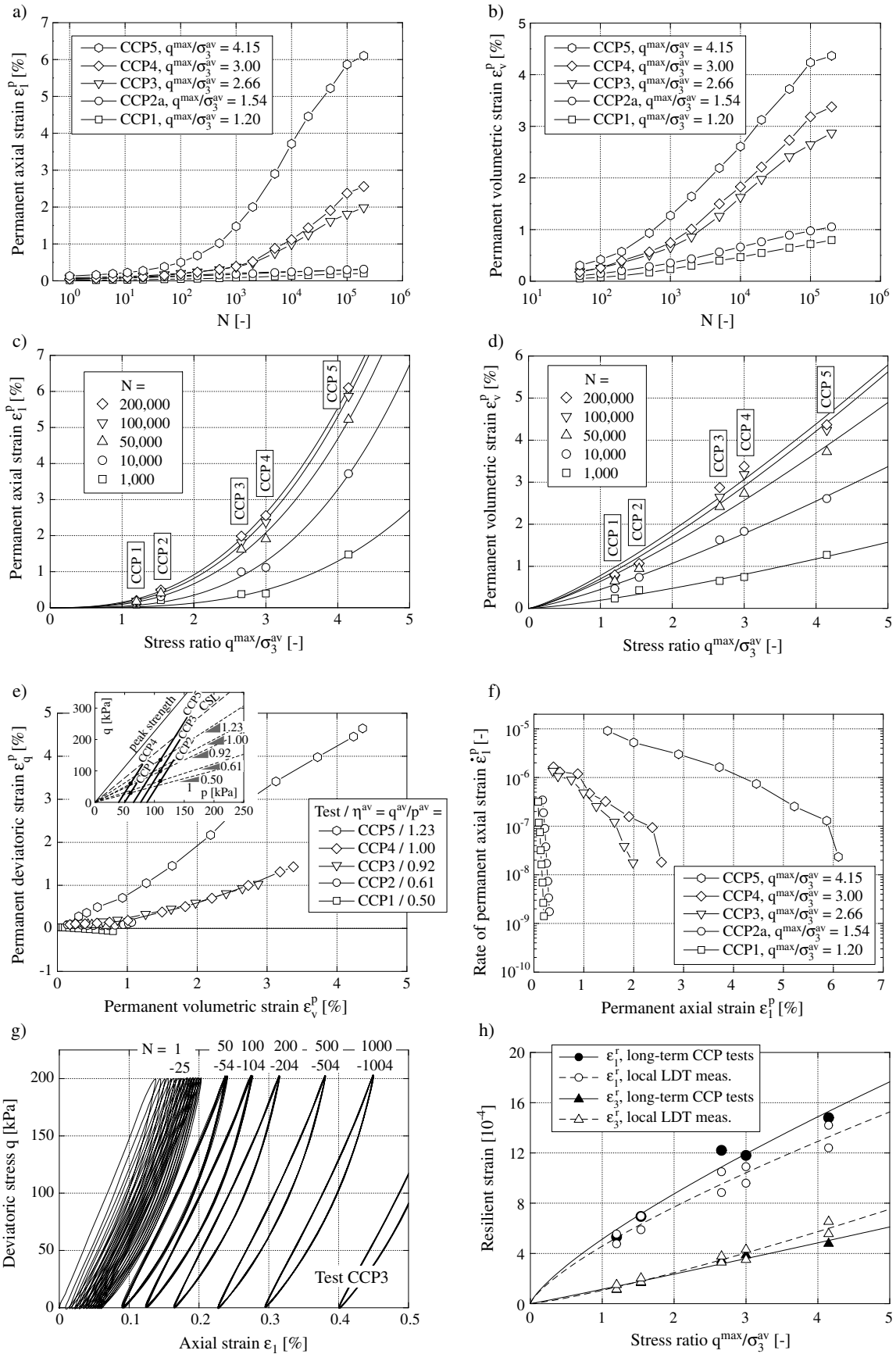Fig. 10: Results of the CCP tests: a) ε_1^p versus N, b) $\varepsilon_v^p(N)$ versus N, c) ε_1^p versus $q^{\max}/\sigma_3^{av}$, d) ε_v^p versus $q^{\max}/\sigma_3^{av}$, e) ε_q^p versus ε_v^p, f) $\dot{\varepsilon}_1^p$ versus ε_1^p g) q-ε_1-hystereses, h) resilient strain ε_1^r versus $q^{\max}/\sigma_3^{av}$

Test	$p^{\min}$ [kPa]	$p^{\max}$ [kPa]	p^{av} [kPa]	p^{ampl} [kPa]	$q^{\min}$ [kPa]	$q^{\max}$ [kPa]	q^{av} [kPa]	q^{ampl} [kPa]	η^{ampl} [-]	σ_3^{av} [kPa]	$q^{\max}/\sigma_3^{\mathrm{av}}$ [-]	L [kPa]	f [Hz]	I_{D0} [-]	$\%\varrho_{\mathrm{Pr}}$ [%]
VCP 1	20.0	100.0	60	40	0	60.0	30.0	30.0	0.75	50	1.2	100.0	0.05	1.03	95
VCP 2	20.0	200.0	110	90	0	135.0	67.5	67.5	0.75	87.5	1.5	225.0	0.05	1.05	95
VCP 3	20.0	200.0	110	90	0	202.5	101.25	101.25	1.125	76.25	2.7	270.9	0.05	0.92	93
VCP 4	20.0	100.0	60	40	0	120.0	60.0	60.0	1.50	40	3.0	144.2	0.05	0.99	94
VCP 5	20.0	200.0	110	90	0	270.0	135.0	135.0	1.50	65	4.2	324.5	0.05	0.98	94
CCP 1	50.0	70.0	60	10	0	60.0	30.0	30.0	3.0	50	1.2	63.2	1.00	1.04	95
CCP 2a	87.5	132.5	110	22.5	0	135.0	67.5	67.5	3.0	87.5	1.5	142.3	1.00	1.06	95
CCP 2b	87.5	132.5	110	22.5	0	135.0	67.5	67.5	3.0	87.5	1.5	142.3	1.00	1.07	95
CCP 2c	87.5	132.5	110	22.5	0	135.0	67.5	67.5	3.0	87.5	1.5	142.3	0.05	1.07	95
CCP 2d	87.5	132.5	110	22.5	0	135.0	67.5	67.5	3.0	87.5	1.5	142.3	0.05	1.05	95
CCP 3	76.25	143.8	110	33.8	0	202.5	101.25	101.25	3.0	76.25	2.7	213.5	1.00	1.11	96
CCP 4	40.0	80.0	60	20	0	120.0	60.0	60.0	3.0	40	3.0	126.5	1.00	1.00	94
CCP 5	65.0	155.0	110	45	0	270.0	135.0	135.0	3.0	65	4.2	94.9	1.00	1.12	96

Table 2: Program of the cyclic triaxial tests ($p^{\min}$, $p^{\max}$, p^{av}, p^{ampl} = minimum, maximum, average or amplitude values of mean pressure, $q^{\min}$, $q^{\max}$, q^{av}, q^{ampl} = minimum, maximum, average or amplitude values of deviator stress, $\eta^{\mathrm{ampl}} = q^{\mathrm{ampl}}/p^{\mathrm{ampl}}$ = inclination of the cyclic stress path, σ_3^{av} = average confining stress, $L = \sqrt{(2p^{\mathrm{ampl}})^2 + (2q^{\mathrm{ampl}})^2}$ = length of the cyclic stress path in the p-q-plane, f = frequency, I_{D0} = initial relative density index)

$\dot{\varepsilon}_q^p = 0$ was fulfilled at considerable larger average stress ratios ($\eta^{\mathrm{av}} \approx 0.5$). Thus, the specimen preparation (tamping of UGM compared to pluviation of sand) seems to influence the direction of accumulation $\dot{\varepsilon}_q^p/\dot{\varepsilon}_v^p$ (so-called "cyclic flow rule" [64]). Probably the preparation method induces an anisotropy and the "isotropic" axis is shifted in the stress space. Plotting the strain paths in a ε_1^p-ε_3^p-diagram shows that stress cycles with an average stress close to the p-axis cause a reduction of the sample diameter (positive values of ε_3^p) while the cross section increases (negative values of ε_3^p) with N for larger average stress ratios (e.g. $\eta^{\mathrm{av}} = 1.23$ in test CCP5). The direction of accumulation $\dot{\varepsilon}_q^p/\dot{\varepsilon}_v^p$ for an UGM under cyclic loading will be the subject of further experimental studies in future.

Fig. 10f shows that the decrease of the rate of permanent vertical strain $\dot{\varepsilon}_1^p$ with the permanent strain ε_1^p itself is faster for low values of the ratio $q^{\max}/\sigma_3^{\mathrm{av}}$. The data points in Fig. 10f refer to $N \geq 1000$. For low stress levels $q^{\max}/\sigma_3^{\mathrm{av}} = 1.20$ and 1.54 the granular material reaches a state called "Shakedown" where the rate of permanent strain accumulation is very small. According to [2] a shakedown is reached if the increment $\Delta\varepsilon_1^p$ between $N = 3000$ and $N = 5000$ is smaller than $4.5 \cdot 10^{-5}$. For the present tests with $q^{\max}/\sigma_3^{\mathrm{av}} = 1.20$ and 1.54 the criterium is fulfilled.

The banana-shaped q-ε_1-hystereses are given exemplary for test CCP3 in Fig. 10g. The early stage of the test ($N \leq 1,000$) is shown. The shape of the hystereses does not significantly change with the number of cycles. The hystereses observed in the CCP and in the VCP tests will be compared later.

The resilient axial strain $\varepsilon_1^r = 2\varepsilon_1^{\mathrm{ampl}}$ and the resilient lateral strain $\varepsilon_3^r = 2\varepsilon_3^{\mathrm{ampl}}$ are plotted versus the stress ratio $q^{\max}/\sigma_3^{\mathrm{av}}$ in Fig. 10h. The filled symbols correspond to the measurements in the long-term CCP tests, that means the measurements of axial deformation with the displacement transducer (corrected by system compliance) and of volumetric deformation using the pipette system. The strains shown as void symbols were derived from the LDT measurements in the two additional tests. The ε_1^r-data is averaged from the values of the two vertical LDTs and the ε_3^r-data is presented as a mean value of the measurements with the eight horizontal LDTs. The data from both (corrected) total and local measurements coincide quite well. The under-linear curve $\varepsilon_1^r(q^{\max}/\sigma_3^{\mathrm{av}})$ in Fig. 10h is due to the stress-dependence of the resilient modulus E_r which is

defined as

$$E_r = \frac{\sigma_1^{\max} - \sigma_1^{\min}}{\varepsilon_1^{\max} - \varepsilon_1^{\min}} = \frac{2q^{\mathrm{ampl}}}{\varepsilon_1^r} \qquad (1)$$

It can be approximated by $E_r \sim (\theta^{\mathrm{av}})^n$ with $n = 0.75$ and $\theta^{\mathrm{av}} = 3p^{\mathrm{av}}$ being the sum of the average principal stresses.

Beside an influence of the average stress, the increase of the accumulation rate with an increasing ratio $q^{\max}/\sigma_3^{\mathrm{av}}$ (Fig. 10c,d) is mainly due to the increase of the strain amplitude (Fig. 10h).

7 VCP test results

Fig. 11a presents the increase of the permanent axial strain with the number of cycles N in the VCP tests. In order to describe the dependence of ε_1^p on the VCP stress path, Brown & Hyde [12] used the ratio $q^{\max}/\sigma_3^{\mathrm{av}}$. From the diagram in Fig. 11c it becomes clear that the data points cannot be described by a unique function $\varepsilon_1^p(q^{\max}/\sigma_3^{\mathrm{av}})$. As an alternative the longitude of the stress path

$$L = \sqrt{(q^{\max} - q^{\min})^2 + (p^{\max} - p^{\min})^2}$$
$$= \sqrt{(2q^{\mathrm{ampl}})^2 + (2p^{\mathrm{ampl}})^2} \qquad (2)$$

may be used, although it does not supply an information about the stress path inclination $\eta^{\mathrm{ampl}} = q^{\mathrm{ampl}}/p^{\mathrm{ampl}}$. Fig. 11d shows that ε_1^P correlates better with L than with $q^{\max}/\sigma_3^{\mathrm{av}}$. However, the permanent strain seems to increase with the stress path inclination η^{ampl}. An increase of the accumulation rate with increasing stress path inclination $q^{\mathrm{ampl}}/p^{\mathrm{ampl}}$ was also reported by Gidel et al. [22] and Habiballah & Chazallon [24]. Thus, both quantities, L and η^{ampl}, are necessary as influencing parameters in empirical equations for ε_1^P.

The permanent volumetric strains, given in Figures 11b as a function of N, can be better understood by looking at the ε_q^p-ε_v^p-diagram in Fig. 11e. For the tests VCP1, VCP3 and VCP5 with large amplitudes ($p^{\max} = 200$ kPa) the ratio $\dot{\varepsilon}_q^p/\dot{\varepsilon}_v^p$ increases with increasing stress path inclination η^{ampl} (i.e. with increasing average stress ratio $\eta^{\mathrm{av}} = q^{\mathrm{av}}/p^{\mathrm{av}}$). The tendency is similar as in the CCP tests. For $\eta^{\mathrm{av}} = 0.5$ the accumulation is almost pure volumetric ($\dot{\varepsilon}_q^p = 0$). Small η^{ampl}-values lead to a decrease of the sample diameter (positive values of ε_3^p) while large ones cause an increase. The test VCP2 with a small amplitude ($p^{\max} = 100$ kPa) at $\eta^{\mathrm{ampl}} = 0.5$ shows the same direction
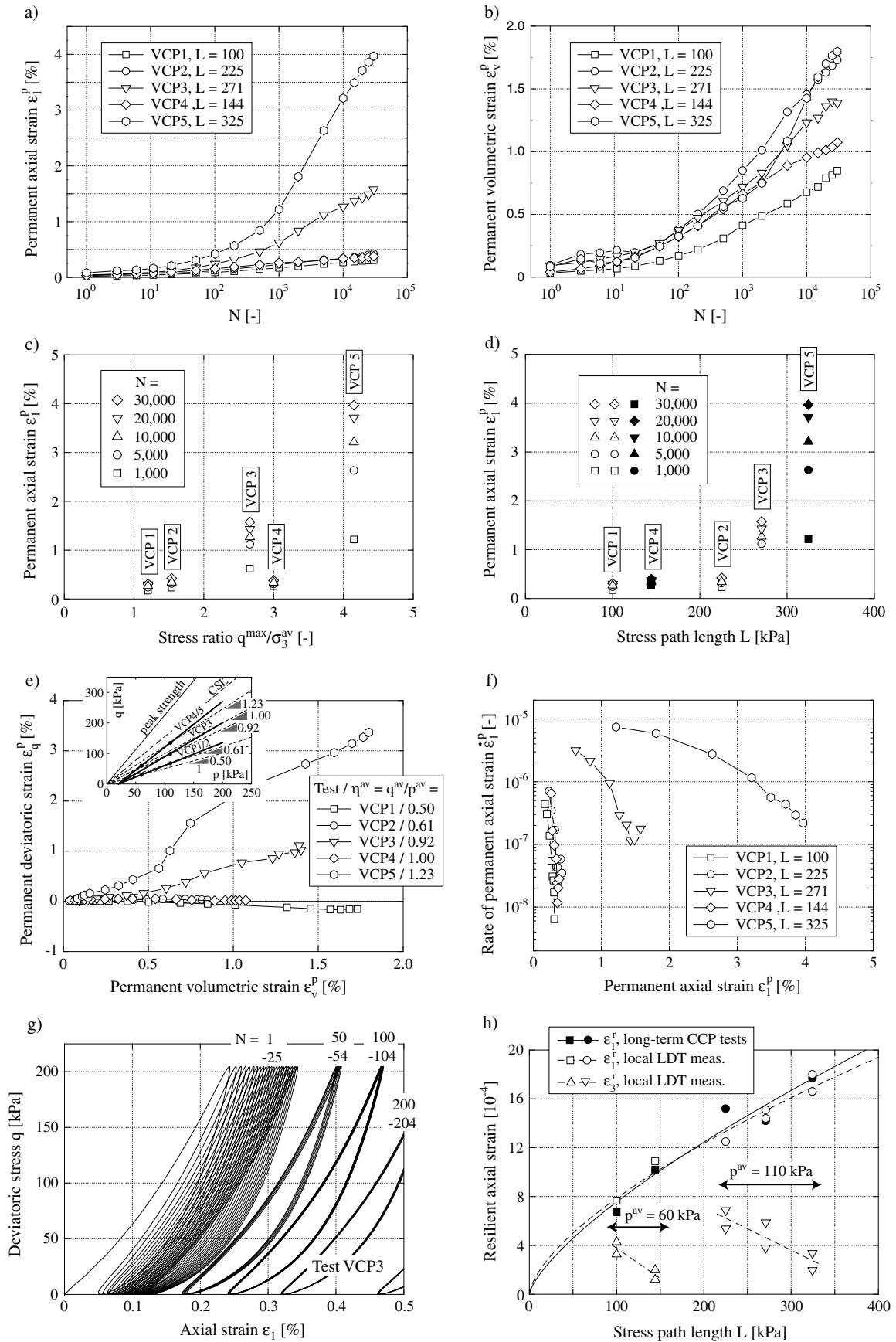
Fig. 11: Results of VCP tests: a) ε_1^p versus N, b) ε_v^p versus N, c) ε_1^p as a function of stress ratio $q^{\max}/\sigma_3^{av}$, d) ε_1^p as a function of the length L of the stress path (empty symbols: stress path inclination $\eta^{ampl} = q^{ampl}/p^{ampl} = 0.75$, symbols with dot: $\eta^{ampl} = 1.125$, filled symbols: $\eta^{ampl} = 1.5$), e) ε_q^p versus ε_v^p, f) $\dot{\varepsilon}_1^p$ versus ε_1^p, g) q-ε_1-hystereses, h) resilient strain ε_1^r versus $q^{\max}/\sigma_3^{av}$

of accumulation as the test VCP1 with the same η^{ampl}-value but with a larger amplitude. However, the small cycles at $\eta^{\text{ampl}} = 1.5$ (test VCP4) also cause an almost volumetric accumulation ($\dot{\varepsilon}_q^p \approx 0$), although a much larger ratio $\dot{\varepsilon}_q^p / \dot{\varepsilon}_v^p$ was observed for the large amplitudes with the same η^{ampl}-value (test VCP5). These effects may be due to an anisotropy of the sample induced by the preparation procedure. Further studies on the direction of accumulation $\dot{\varepsilon}_q^p / \dot{\varepsilon}_v^p$ of pre-compacted UGM materials are necessary.

Looking at Fig. 11b, there are two effects that affect the rate of volumetric strain accumulation. First, the plastic volumetric strain increases with the amplitude (longitude) of the stress path (ε_v^p in tests Nos. VCP2 and VCP5 with large amplitudes is larger than in tests Nos. VCP1 and VCP4 with same η^{ampl} but with smaller amplitudes). Second, the ratio of the rates of deviatoric and volumetric strain accumulation $\dot{\varepsilon}_q^p / \dot{\varepsilon}_v^p$ increases with increasing average stress ratio η^{av} (or with increasing stress path inclination η^{ampl}, respectively). Both effects are counteracting.

In a similar way to the CCP tests, the rate of permanent axial strain decreases with an increase of the permanent strain itself (Fig. 11f). The data points in Fig. 11f refer to $N \geq 1,000$. The decrease of the rate is faster for the smaller amplitudes. The criteria for a shakedown [2] are fulfilled for none of the VCP tests.

Fig. 11g shows the q-ε_1-hystereses in the test VCP3 for $N \leq 100$. Similar to the hystereses in the CCP tests (Fig. 10g) they have a banana-like shape. The scale of the ε_1-axis is the same as in Fig. 10g in order to compare the area encompassed by the hystereses in the q-ε_1-diagram. It is larger for VCP stress paths than for CCP ones.

Fig. 11h presents the increase of the resilient strain ε_1^r with stress path length L. The values obtained from the long-term tests coincide well with the additional LDT measurements. The increase of the accumulation rate with L (Fig. 11c) is mainly due to the accompanying increase of the strain amplitude (Fig. 11h). Due to membrane penetration the values $\varepsilon_3^r = 0.5(\varepsilon_v^r - \varepsilon_1^r)$ in the VCP long-term tests are not reliable. The LDT measurements show that for a constant p^{av} the lateral resilient strain decreases approximately linear with increasing stress path inclination $\eta^{\text{ampl}} = q^{\text{ampl}}/p^{\text{ampl}}$. This is due to the decreasing distance to the critical state line. For $\eta^{\text{ampl}} = $ constant, ε_3^r increases with increasing amplitude of the cycles.

8   Comparison of CCP and VCP test results

A comparison of the residual axial strains after $N = 20,000$ cycles in CCP and VCP tests is presented in Fig. 12a (which is similar to Fig. 3 of Brown & Hyde [12]). Except for the tests VCP4 and CCP4, the absolute differences in the ε_1^p-values between the CCP and the VCP tests seem to be small. Fig. 12b contains a plot of ε_v^p versus $q^{\text{max}}/\sigma_3^{\text{av}}$. For small stress ratios $q^{\text{max}}/\sigma_3^{\text{av}} \leq 1.5$ the VCP tests deliver significantly larger volumetric strains than the corresponding CCP tests. The behaviour is opposite for the larger tested stress ratios $q^{\text{max}}/\sigma_3^{\text{av}} \geq 2.7$.

The differences, especially for the smaller amplitudes, become clearer from the left column of diagrams in Fig. 13 showing ε_1^p versus N. Comparing VCP tests Nos. 1 and 2 with $\eta^{\text{ampl}} = 0.75$ with the respective CCP tests (Figures 13a,d) the permanent axial strain was larger in the VCP tests. After $N = 20,000$ cycles the permanent axial strain ε_1^p in the test VCP1 was 1.8 times larger than that in the

test CCP1. This factor was 1.6 for tests CCP2 and VCP2. In the test VCP3 with $\eta^{\text{ampl}} = 1.125$ (Fig. 13g) the residual axial strain was similar as in the corresponding CCP test (factor 1.1 between ε_1^p in the VCP and in the CCP test at $N = 20,000$). When a stress path with $\eta^{\text{ampl}} = 1.50$ was applied in the VCP tests the behavior depended on the amplitude. For a small amplitude (tests No. 4, Fig. 13j) the UGM experienced a larger permanent strain in the CCP test and the differences significantly increased with N (factor 4.1 between ε_1^p in the CCP and in the VCP test at $N = 20,000$). There is no significant difference in the ε_1^p-values in the case of a large amplitude (tests No. 5, Fig. 13m, factor 1.2 between ε_1^p in the CCP and in the VCP test at $N = 20,000$). Thus, CCP and VCP tests seem to deliver similar permanent axial strains ε_1^p for stress paths with intermediate and large stress path inclinations $1.125 \leq \eta^{\text{ampl}} \leq 1.5$ as long for the latter case the amplitudes are large. The assumption of Brown & Hyde [12] that the permanent axial strain is not affected by the type of test is disproved for some of the tested stress paths. Especially for low stress path inclinations $\eta^{\text{ampl}} = 0.75$ it is not on the safe side.
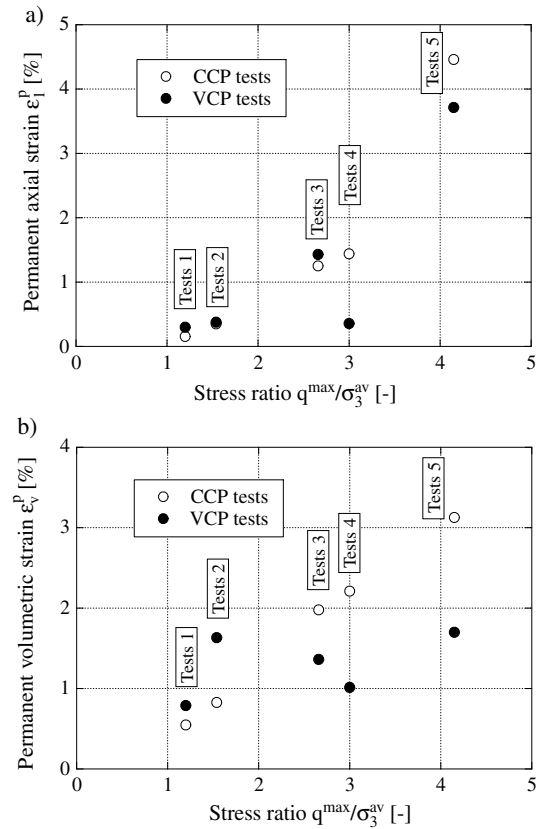

Fig. 12: a) Permanent axial strain and b) permanent volumetric strain after $N = 2 \cdot 10^4$ cycles versus stress ratio $q^{\text{max}}/\sigma_3^{\text{av}}$

The permanent volumetric strains are compared in the middle column of diagrams in Fig. 13. While VCP stress paths with small inclinations $\eta^{\text{ampl}} = 0.75$ delivered larger rates of volume changes than the corresponding CCP tests (Fig. 13b,e), the behavior was opposite for intermediate and large stress path inclinations (Fig. 13h,k,n), especially for large numbers of cycles. The distance of the maximum stress to the CSL may play a role.

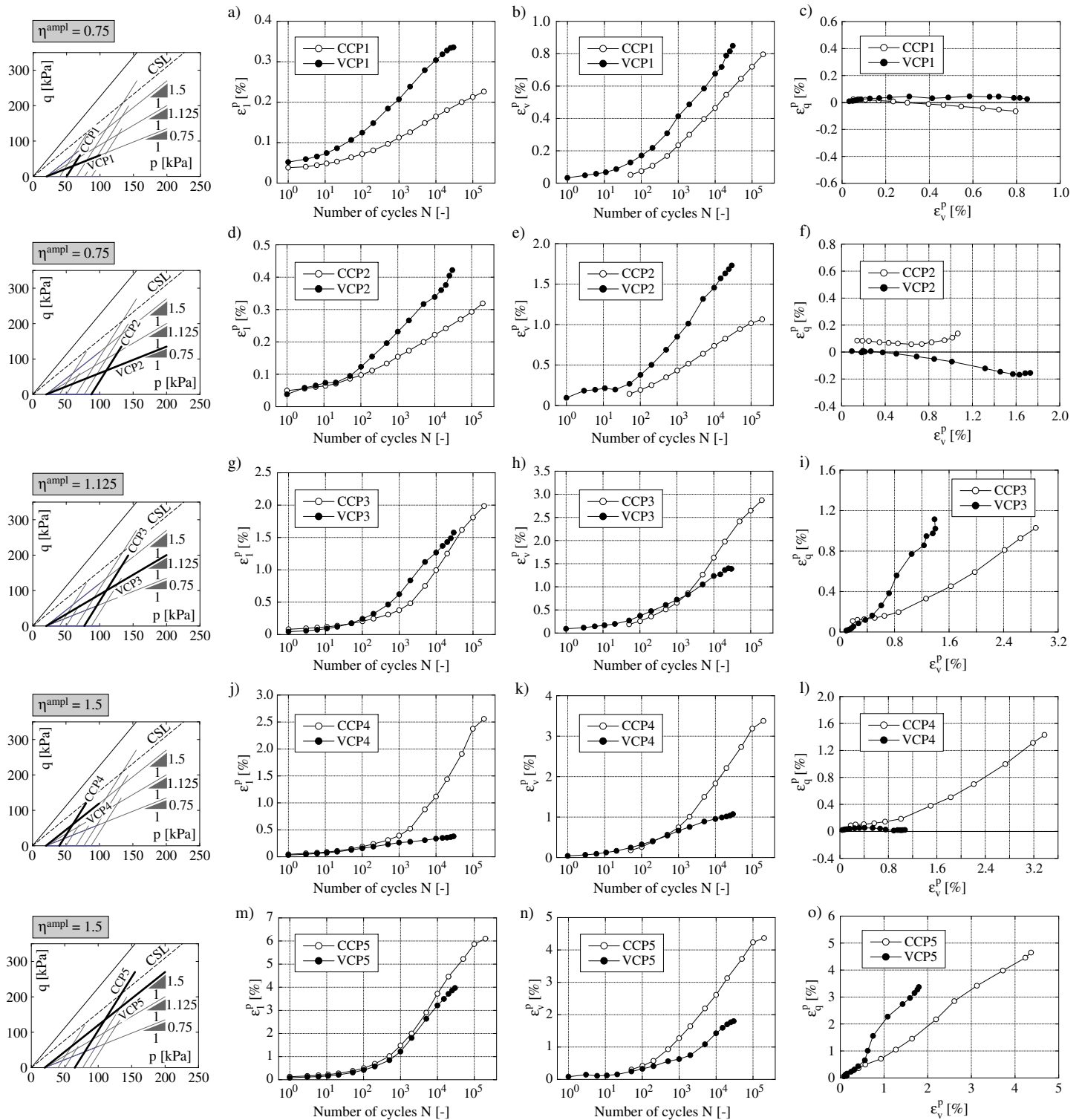The ε_q^p-ε_v^p-strain paths on the right side of Fig. 13 show

Fig. 13: *Permanent axial and volumetric strain versus number of load cycles, permanent deviatoric versus permanent volumetric strain: comparison of CCP and VCP tests*

a quite similar direction of accumulation $\dot{\varepsilon}_q^p/\dot{\varepsilon}_v^p$ in CCP and VCP tests for small VCP stress path inclinations (Fig. 13c,f). For intermediate and large η^{ampl}-values combined with large stress amplitudes (Fig. 13i,o), the deviatoric portion of the direction of accumulation was significantly larger in the VCP tests than in the corresponding CCP tests (although the average stress ratios η^{av} were equal).

For small and intermediate values $0.75 \leq \eta^{\mathrm{ampl}} \leq 1.125$, the VCP stress paths caused larger resilient axial strains ε_1^r than the CCP ones. For large VCP stress path inclinations $\eta^{\mathrm{ampl}} = 1.5$, the amplitudes of axial strain were quite similar in both types of tests.

Summary and conclusions

Several pairs of cyclic triaxial tests with (VCP tests) and without (CCP tests) a variation of the confining pressure have been performed on an unbound granular material in order to compare the residual deformations in both types of tests. The present study demonstrates, that for most of the tested stress paths CCP and VCP tests with equal average stress $\boldsymbol{\sigma}^{\mathrm{av}}$ and equal amplitude of deviatoric stress q^{ampl} deliver different permanent and resilient strains. For some special stress paths, some of the components of strain may be equal in CCP and VCP tests (e.g. ε_1^p for intermediate or large VCP stress path inclinations η^{ampl} and large amplitudes).

For the design of pavements, the permanent axial strain is the most important strain component. For small values of the VCP stress path inclination $\eta^{\mathrm{ampl}} = q^{\mathrm{ampl}}/p^{\mathrm{ampl}} = 0.75$ the residual axial strain in the VCP tests was larger than in the corresponding CCP test, independently of the applied amplitude. If VCP cycles were applied along an intermediate inclination $\eta^{\mathrm{ampl}} = 1.125$ the residual strains in VCP and CCP tests were similar. The same applies to large VCP stress path inclinations $\eta^{\mathrm{ampl}} = 1.5$ in combination with large amplitudes. For $\eta^{\mathrm{ampl}} = 1.5$ and smaller amplitudes the residual strain in the CCP test exceeded the one of the corresponding VCP test. Thus, the present work disproves the assumption that VCP and CCP tests generally deliver similar results.

Since small values of η^{ampl} are realistic for pavements, CCP tests seem to underestimate the residual axial strain in comparison to VCP tests. Thus, VCP tests should be preferred to CCP ones. However, it has to be kept in mind that both, CCP and VCP tests cannot simulate the shear stress component during the cycles and thus both may underestimate the accumulation rates observed in situ.

References

[1] The Asphalt Institute - TAI. Research and Development of the Asphalt Institute's Thickness Design Manual MS - 1, 9th Ed., College Park, Md., 1982.

[2] DIN EN 13286-7: Triaxial tests with cyclic loading for unbound granular material, 2004.

[3] A. Adu-Osei, D. N. Little, and R. L. Lytton. Cross-anisotropic Characterization of Unbound Granular Materials. Transportation Research Record, 1757:82 – 91, 2001.

[4] J. J. Allen and M. R. Thompson. Resilient Response of Granular Materials Subjected to Time-Dependent Lateral Stresses. Transportation Research Record, 510:1 – 13, 1974.

[5] R. D. Barksdale. Performance of Crushed-Stone Base Courses. Transportation Research Record, 954:78 – 87, 1984.

[6] R. D. Barksdale and R. G. Hicks. Material Characterization and Layered Theory for use in Fatigue Analysis. HRB Special Report, 140:20 – 48, 1973.

[7] R.D. Barksdale. Laboratory evaluation of rutting in base course materials. In Third International Conference on Structural Design of Asphalt Pavements, volume 3, pages 161–174, 1972.

[8] R. Bonaquist. Summary of Pavement Performance Test Using the Accelerated Loading Facility, 1986 - 1990. Transportation Research Record, 1354:74 – 85, 1992.

[9] H. R. Boyce. A Non-linear Model for the Elastic Behaviour of Granular Materials Under Repeated Loading. In Proceedings International Symposium on Soils under Cyclic and Transient Loading, Swansea, U.K., volume 1, pages 285–294, 1980.

[10] J. R. Boyce. The Behaviour of a Granular Material under Repeated Loading. PhD thesis, University of Nottingham, 1976.

[11] S. F. Brown. Repeated Load Testing of a Granular Material. Journal of the Geotechnical Engineering Division, ASCE, 100(7):825 – 841, 1974.

[12] S. F Brown and A. F. L. Hyde. Significance of Cyclic Confining Stress in Repeated-load Triaxial Testing of Granular Material. Transportation Research Record, 537:49 – 58, 1975.

[13] S. F. Brown and P. S. Pell. An Experimental Investigation of the Stresses, Strains and Deflections in a Layered Pavement Structure Subjected to Dynamic Loads. In Proc. 2nd Int. Conf. Struct. Des. of Asphalt Pavements, pages 487–504, 1967.

[14] S. F. Brown and E. T. Selig. Cyclic loading of soils, chapter The Design of Pavement and Rail Track Foundations, pages 249 – 305. 1991.

[15] S.F. Brown. Soil Mechanics in Pavement Engineering. The 36th Rankine Lecture of the British Geotechnical Society. Géotechnique, 46(3):383 – 426, 1996.

[16] F. W. K. Chan and S. F. Brown. Significance of Principal Stress Rotation in Pavements. In XIII ICSMFE, New Delhi, India, pages 1823 – 1826, 1994.

[17] I. F. Collins and M. Boulbibane. Geomechanical Analysis of Unbound Pavements Based on Shakedown Theory. Journal of Geotechnical and Geoenvironmental Engineering, ASCE, 126:50 – 59, 2000.

[18] Shell International Petroleum Company. Shell Pavement Design Manual - Asphalt Pavement and Overlays for Road Traffic, London. , 1978.

[19] A. R Dawson, M J Mundy, and M. Huhtala. European Research into Granular Material for Pavement Bases and Subbases. Transportation Research Record, pages 91–99, 2000.

[20] INVIAS Instituto Nacional de Vías. Especificaciones generales de construcción de carreteras. Bogotá D.C., Colombia, 2002.

[21] P. A. Garnica, G. N. Pérez, and L. A. Gomes. Módulo de Resiliencia en Suelos Finos y Materiales Granulares. Secretaría de Comunicaciones y Transportes (SCI). Technical Report 142, Instituto Mexicano del Transporte (IMT). Sanfandila, México, 2001.

[22] G. Gidel, D. Breysee, P. Hornych, J.-J. Chauvin, and A. Denis. A new approach for investigating the permanent deformation behaviour of unbound granular material using the repeated load triaxial apparatus. *Bulletin des Laboratoires des Ponts et Chaussées*, 233(4):5–21, 2001.

[23] S. Goto, F. Tatsuoka, S. Shibuya, Y.-S. Kim, and T. Sato. A simple gauge for local small strain measurements in the laboratory. *Soils and Foundations*, 31(1):169–180, 1991.

[24] T. Habiballah and C. Chazallon. An Elastoplastic Model Based on the Shakedown Concept for Flexible Pavements Unbound Granular Materials. *Int. J. Numer. Anal. Meth. Geomech.*, 29:577–596, 2005.

[25] T. Habiballah, C. Chazallon, and P. Hornych. Simplified Model Based on the Shakedown Theory for Flexible Pavements. In *Proc. of the 6th International Symposium on Pavements Unbound*, pages 191 – 198, 2004.

[26] P. Y Hicher and C. S. Chang. Anisotropic Nonlinear Elastic Model for Particulate Materials. *Journal of Geotechnical and Geoenvironmental Engineering, ASCE*, 132(8):1052 – 1061, 2006.

[27] R. G. Hicks and C. L. Monismith. Prediction of the Resilient Response of Pavements Containing Granular Layers Using Non-linear Elastic Theory. In *Proceedings of the 3rd International Conference on Asphalt Pavements*, volume 1, pages 410–429, 1972.

[28] I. Hoff and R. S. Nordal. Constitutive Model for Unbound Granular Materials Based in Hyperelasticity. In Gomes Correia, editor, *Unbound Granular Materials - Laboratory Testing, In-situ Testing and Modelling*, pages 187–196. Balkema, Rotterdam, 1999.

[29] E. Hoque, T. Sato, and F. Tatsuoka. Performance evaluation of LDTs for use in triaxial tests. *Geotechnical Testing Journal, ASTM*, 20(2):149–167, 1997.

[30] M. Huurman. *Permanent deformation in concrete block pavements*. PhD thesis, Delft University of Technology, 1997.

[31] A.F.L. Hyde. *Repeated load triaxial testing of soils*. PhD thesis, University of Nottingham, 1974.

[32] IDU. Instituto de Desarrollo Urbano and Universidad de Los Andes, Manual de Diseno de Pavimentos para Bogotá. Bogotá D.C., Colombia. , 2002.

[33] T. Ingason, L. G. Wiman, and H. Haraldsson. HVS - Testing of Iceland Low Volume Road Structures. In *ISAP - 9th International Conference on Design of Asphalt Pavements*, 2002.

[34] K. Ishihara and S. Yasuda. Sand liquefaction due to irregular excitation. *Soils and Foundations*, 12(4):65–77, 1972.

[35] I. V. Kalcheff and R. G. Hicks. A Test Procedure for Determining the Resilient Properties of Granular Materials. *Journal of Testing and Evaluation*, 1(6):472 – 479, 1973.

[36] P. Kolisoja, T. Saarenketo, H. Peltoniemi, and N. Vuorimies. Laboratory Testing of Suction and Deformation Properties of Base Course Aggegates. *Transportation Research Record*, 1787:83 – 89, 2002.

[37] TRL Transport Research Laboratory. A Guide to the Structural Design of Bitumen-Surfaced Roads in Tropical and Sub-tropical Countries. RN31, Draft 4th edition. , 1993.

[38] F. Lekarp, U. Isacsson, and A. Dawson. State of the art. I: Resilient response of unbound aggregates. *Journal of Transportation Engineering*, 126(1):66–75, 2000.

[39] F. Lekarp, I. R. Richardson, and A. Dawson. Influences on Permanent Deformation Behavior of Unbound Granular Materials. *Transportation Research Record*, 1547:68 – 75, 1996.

[40] J. R. Morgan. The Response of Granular Materials to Repeated Loading. In *Proc., 3rd Conf., ARRB*, 1966.

[41] A. Nataatmadja and A. K. Parkin. Characterization of Granular Materials for Pavements. *Canadian Geotechnical Journal*, 26:725 – 730, 1989.

[42] P.G. Nicholson, R.B. Seed, and H.A. Anwar. Elimination of membrane compliance in undrained triaxial testing. I. Measurement and evaluation. *Canadian Geotechnical Journal*, 30:727–738, 1993.

[43] American Association of State Highway and Transportation Officials (AASHTO). Guide for Design of Pavement Structures, Washington, D. C. , 1993.

[44] J.-L. Paute, A. R. Dawson, and P. J. Galjaard. Recommendations for Repeated Load Triaxial Test Equipment and Procedure for Unbound Granular Materials. In Gomes Correia, editor, *Flexible Pavement*, pages 23 – 34. Balkema, Rotterdam, 1996.

[45] B. D. Pidwerbesky. *Fundamental Behaviour of Unbound Granular Pavements Subjected to Various Loading Conditions and Accelerated Trafficking*. PhD thesis, University of Canterbury, Christchurch, New Zealand, 1996.

[46] R. Pyke, H.B. Seed, and C.K. Chan. Settlement of sands under multidirectional shaking. *Journal of the Geotechnical Engineering Division, ASCE*, 101(GT4):379–398, 1975.

[47] C. Rada and W. M. Witczak. Comprehensive Evaluation of Laboratory Resilient Moduli Results for Granular Materials. *Transportation Research Record*, 810:23 – 33, 1981.

[48] H. A. Rondón and A. Lizcano. Modelos de comportamiento de materiales granulares para pavimentos y aplicación de la ley constitutiva hipoplástica. In *III Jornadas Internacionales de Ingeniera Civil. Cuba*, 2006.

[49] H. A. Rondón, T. Wichtmann, Th. Triantafyllidis, and A. Lizcano. Hypoplastic material constants for a well-graded granular material for base and subbase layers of flexible pavements. *Acta Geotechnica*, 2(2):113–126, 2007.

[50] G.T.H. Sweere. *Unbound granular bases for roads*. PhD thesis, Delft University of Technology, Netherlands, 1990.

[51] E. Taciroglu and K. D. Hjelmstad. Simple Nonlinear Model for Elastic Response of Cohesionless Granular Materials. *Journal of Engineering Mechanics*, 128:969 – 978, 2002.

[52] F. Tatsuoka, M. Ishihara, T. Uchimura, and A. Gomes Correia. Non-linear Resilient Behaviour of Unbound Granular Materials Predicted by the Cross-Anisotropic Hypo-Quasi-Elasticity Model. In Gomes Correia, editor, *Unbound Granular Materials - Laboratory testing, In-situ testing and modelling*, pages 197–206. Balkema, Rotterdam, 1999.

[53] H. L. Theyse. Stiffness, Strength, and Performance of Unbound Aggregate Materials: Application of South African HVS and Laboratory Results to California Flexible Pavements. Report produced under the auspices of the California Partnered Pavement Research Program for the California Department of Transportation. Technical report, University of California, 2002.

[54] N. H. Thom and S. F. Brown. Effect of Moisture on the Structural Performance of a Crushed-Limestone Road Base. *Transportation Research Record*, 1121:50 – 56, 1987.

Wichtmann & Triantafyllidis

J. Transp. Eng., ASCE, Vol. 135, No. 7, pp. 467-478, 2009

[55] N. H. Thom and A. R. Dawson. The Permanent Deformation of a Granular Material Modelled Using Hollow Cylinder Testing. In Gomes Correia, editor, *Flexible Pavement*, pages 65 – 78. Balkema, Rotterdam, 1996.

[56] M. R. Thompson and K. L. Smith. Repeated Triaxial Characterization of Granular Bases. *Transportation Research Record*, 1278:7 – 17, 1990.

[57] K. H. Tseng and R. L. Lytton. Prediction of Permanent Deformation in Flexible Pavement Materials. *Journal Assoc. Asphalt Paving Technol.*, 58:155 – 156, 1989.

[58] E. Tutumluer and M. R. Thompson. Anisotropic Modelling of Granular Bases in Flexible Pavements. *Transportation Research Record*, 1577:18 – 26, 1997.

[59] J. Uzan. Granular Material Characterization for Mechanistic Pavement Design. *Journal of Transportation Engineering*, 125:108 – 113, 1999.

[60] J. Uzan. Permanent Deformation in Flexible Pavements. *Journal of Transportation Engineering*, 130:6 – 13, 2004.

[61] S. Werkmeister. *Permanent Deformation Behaviour of Unbound Granular Materials in Pavement Constructions.* PhD thesis, University of Technology, Dresden, 2003.

[62] S. Werkmeister, A. Dawson, and F. Wellner. Pavement Design Model of Unbound Granular Materials. *Journal of Transportation Engineering*, 130:665 – 674, 2004.

[63] S. Werkmeister, R. Numrich, A. Dawson, and F. Wellner. Deformation Behaviour of Granular Materials under Repeated Dynamic Load. *Journal of Environmental Geomechanics - Monte Verit*, 2002.

[64] T. Wichtmann, A. Niemunis, and T. Triantafyllidis. Strain accumulation in sand due to cyclic loading: drained triaxial tests. *Soil Dynamics and Earthquake Engineering*, 25(12):967–979, 2005.

[65] T. Wichtmann, A. Niemunis, and T. Triantafyllidis. On the influence of the polarization and the shape of the strain loop on strain accumulation in sand under high-cyclic loading. *Soil Dynamics and Earthquake Engineering*, 27(1):14–28, 2007.

[66] T.L. Youd. Compaction of sands by repeated shear straining. *Journal of the Soil Mechanics and Foundations Division, ASCE*, 98(SM7):709–725, 1972.

[67] D. Zaman, M.and Chen and J. Laguros. Resilient Moduli of Granular Materials. *Journal of Transportation Engineering*, 120(6):967 – 988, 1994.